

Towards Robot-Assisted Post-Stroke Hand Rehabilitation: Fugl-Meyer Gesture Recognition Using sEMG

Miao Chen, Long Cheng, Fubiao Huang, Yan Yan, and Zeng-Guang Hou

Abstract—Robot-assisted rehabilitation training requires to identify the patient's motion intention effectively. These motions are usually originated from rehabilitation actions included in the Fugl-Meyer assessment scale. Surface electromyography (sEMG) is the most commonly used physiological signal for identifying the motion intention of patients. The use of sEMG to classify different gesture patterns is one key technology for the human-machine interaction. Therefore, this paper investigates a Fugl-Meyer hand gesture recognition method towards robot-assisted hand rehabilitation. The experiment data set including eight hand gesture information is collected from six volunteers. Six single features (Difference Absolute Mean Value (DAMV), Integral of Absolute Value (IAV), Variance (VAR), Autoregressive Coefficients (AR), maximum value of Discrete Wave Transformation (DWTmax) and standard deviation of Discrete Wavelet Transform (DWTstd)) are used to recognize the gesture. The experimental results demonstrate that: (1) a segment length of 250 ms contains enough information to estimate the hand gestures and leaves sufficient time to do feature extraction and gesture recognition; (2) by comparing the performance of different single features, DWTstd wins the highest accuracy (i.e., 96%); (3) the combination of single features into a multi-feature can effectively improve the recognition accuracy, where the best performance is achieved by multi-feature combining DAMV, IAV and AR under BP neural network classifier (the average accuracy is 97.71%); (4) as to different classifiers, BP neural network has a better performance than Support Vector Machine (SVM) and Extreme Learning Machine (ELM).

Index Terms—surface electromyography (sEMG), gesture recognition, Fugl-Meyer assessment scale (FMAS), hand rehabilitation, back propagation neural network (BPNN).

I. INTRODUCTION

Recently, American Heart Association has reported that approximately 700,000 people experience a new or recurrent stroke in the United States each year [1]. The neurological damage caused by the stroke and motor impairment often greatly affects and limits the quality and autonomy of life, while hand function impairment is one of the most serious issues after neurological damage [2] (two thirds of stroke survivors suffer from partial paralysis at the level of the arm and hand [3]). While hand is irreplaceable in daily life, regaining hand and arm function was identified as the most critical need for people with paralyzed limbs [4].

This work was supported in part by the National Natural Science Foundation of China (Grants 61422310, 61633016, 61370032) and Beijing Natural Science Foundation (Grant 41620667).

Miao Chen, Long Cheng, Yan Yan and Zeng-Guang Hou are with the State Key laboratory of Management and Control for Complex Systems, Institute of Automation, Chinese Academy of Sciences, Beijing 100190, China. Email: long.cheng@ia.ac.cn. Miao Chen and Long Cheng are also with the University of Chinese Academy of Sciences. Fubiao Huang is with Faculty of Rehabilitation, Capital Medical University, Beijing 100068, China.

The treatment of paralysis is a long-term process, which will lead to a large number of medical and human resource consumption [5]. The number of rehabilitation therapists in the world is insufficient to meet the needs in the rehabilitation market. With the development of robots, researchers attempt to use rehabilitation robots to assist patients to do rehabilitation training [6] [7] [8]. In order to realize the communication between the robot and the patient (let the robot understand the current recovery state of the patient), it is necessary to establish an effective human-machine interaction method. At present, the popular physiological signals used to achieve human-machine interaction are EEG, EOG and sEMG, where sEMG is the most commonly used one [9] [10]. The use of sEMG to classify different gesture patterns is one key technology for the human-machine interaction [11]. Therefore, a study on the hand gesture recognition using sEMG has been developed in this paper, which aims to realize an effective interaction between the robot and the patient.

A series of studies have been carried out for the analysis of sEMG. Harrach *et al.* attempted to separate two sEMG activities of the brachialis and the biceps brachii by using a High Density sEMG (HD-sEMG) grid placed at the upper arm. Canonical Component Analysis (CCA) technique was employed for obtaining more accurate and solid results [12]. Winslow *et al.* used a 24-h sEMG recordings to do identification and classification of muscle spasms, which is important for clinical management of spasticity [13]. Ding *et al.* came up with an Extended Full-Dimensional Gaussian Mixture Model to solve sEMG-based motion recognition with incomplete data [14]. Different approaches have been proposed to extract the information of sEMG and different classifiers have been employed to classify hand gestures. Zhai *et al.* utilized the spectrogram of sEMG to do short latency hand movement classification by SVM [15]. Various features such as time domain features, frequency domain features, and other non-linear features are used to classify hand gestures in [16] [17]. Adewuyi *et al.* got an accuracy of 96% for non-amputees and 85% for partial-hand amputees by combining EMG data from both intrinsic and extrinsic hand muscles to classify hand grasps and finger motions with LDA [18]. Duan *et al.* combined the wavelet transform and the back propagation (BP) neural network to recognize the gradual changes of six hand motions, the average accuracy rate is found to be 92.17% [19].

Although many studies have been done to improve the accuracy of hand gesture recognition, most of the gestures are general hand gestures. To the best of the authors' knowledge, there is no study on the hand gesture recognition towards hand rehabilitation training. At present, one method for post-stroke

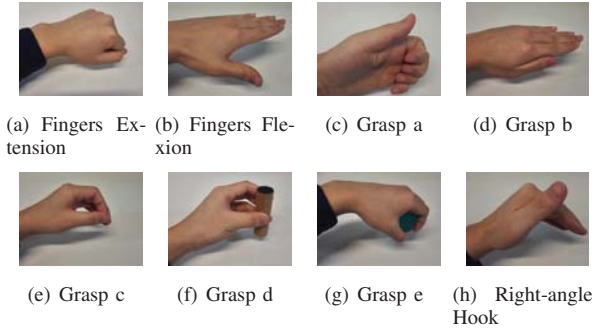


Fig. 1. Eight Fugl-Meyer hand gestures.

hand function rehabilitation is to do separation action. Fugl-Meyer assessment scale is the most widely used method for stroke hemiplegia motor function evaluation. Therapists often use it to help patients do rehabilitation exercise in the clinical practice. Therefore, it is necessary to improve the classification accuracy of Fugl-Meyer hand gesture for ensuring the safety of patients in the process of rehabilitation training. To this end, how to optimal divide the sEMG data into segments for real-time recognition; how to select the features and classifiers must be addressed.

To address these challenges, a study on Fugl-Meyer hand gesture recognition towards robot-assisted post-stroke hand rehabilitation using sEMG has been developed in this paper. Eight hand gestures in the Fugl-Meyer assessment scale have been collected from six volunteers. Then, six features in the time domain, frequency domain and time-frequency domain are used to do feature extraction. Finally, a three-layer BP neural network has been employed to recognize eight hand gestures based on these features.

The rest of this paper is organized as follows. Section II introduces the data acquisition and preprocessing in the experiment. Feature selection and gesture recognition method are described in Section III. Section IV provides the experimental results and their analysis. Finally, Section V concludes the study and presents suggestions for future work.

II. DATA ACQUISITION AND PREPROCESSING

A. Fugl-Meyer Assessment Scale and Hand Gesture

Fugl-Meyer assessment scale is a measure of upper extremity (UE) and lower extremity (LE) motor and sensory impairment. It is the most popular assessment scale used to assess the motor function in clinical applications because of its detailed content, accurate result and short appraise time. All of the hand gestures used in this paper are based on the Fugl-Meyer assessment scale. These gestures are separate gestures often used in the process of rehabilitation. Participants have to perform eight gestures which are shown in Fig. 1 and listed as follows:

1) *Fingers Mass Extension*: full fingers extension active or passive.

2) *Fingers Mass Flexion*: full fingers flexion active or passive.

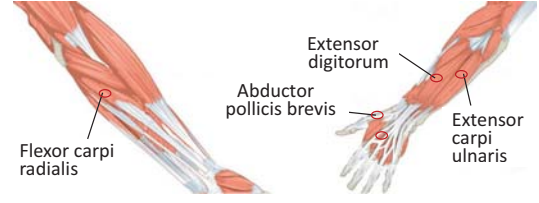


Fig. 2. Muscle positions for the electrode locations.

3) *Grasp a*: hook grasp that extends the metacarpophalangeal joints and flex the proximal and distal interphalangeal joints.

4) *Grasp b*: thumb adduction that four fingers keep straight and abduct the thumb to grasp a piece of paper.

5) *Grasp c*: grasp a pen or pencil by opposing the thumb and index finger pads around the pen.

6) *Grasp d*: cylindrical grasp that the patient can grasp a cylindrical object. This cylindrical object is a stick used in the hand rehabilitation training.

7) *Grasp e*: spherical grip that the patient can grip spherical objects. This spherical object is a ball used in rehabilitation training.

8) *Right-angle Hook*: proximal and distal interphalangeal joints keep extension with metacarpophalangeal joint bending 90 degrees.

B. Experimental Setup

In this experiment, six healthy volunteers including five males (23, 21, 24, 23, and 24 years old) and one female (22 years old) were recruited to execute eight hand gestures which have been introduced in the previous section. The average body height of volunteers is 171.5 cm; the average of body mass is 60 kg. All participants have signed an informed consent prior to the experiments. The equipment of acquiring sEMG signals is a device that was independently designed by Institute of Automation Chinese Academy of Sciences (CASIA). This equipment can collect 8 channels of sEMG simultaneously with a 1024Hz sampling frequency in each channel. The device that runs the sEMG signal acquisition program is a quad-core Intel Core i7 personal computer. According to the musculoskeletal system, flexor carpi radialis, extensor digitorum, extensor carpi ulnaris and abductor pollicis brevis are selected to collect the sEMG. Besides, the muscle which is 1-cm away from the index finger joint is also selected to collect sEMG. The muscle positions for the electrode locations are shown in Fig. 2.

In order to improve the quality of signal acquisition, some pre-experiment preparations were done before patching the electrode: such as scratching the skin hair on the surface of the collected muscle and washing the skin with alcohol.

C. Data Acquisition and Preprocessing

The gestures or the way to grasp objects have been shown to the participants before experiments. Each gesture lasts 2 seconds (2048 points for each channel) and is repeated for 50 times, 3 seconds relax that keeps the hand open and no muscle

activity state is made between every repeat. After a single gesture has been repeated 50 times, rest the hand for 5 minutes to begin the next gesture. This can effectively prevent the muscle fatigue and improve the quality of signal acquisition.

sEMG is a weak electrical signal generated by nervous system stimulating the muscle contraction essentially. The frequency range of sEMG is usually from 10 Hz to 500 Hz. The dominated frequency is within 50-150 Hz. Because the original sEMG is very weak, the data are susceptible to external interferences such as intrinsic noise of electronic components and acquisition equipment, DC baseline noise [20]. Since the noise is mainly concentrated in a low-frequency range from 0 Hz to 20 Hz, a band-pass filter from 20 Hz to 500 Hz is set to eliminate the noise effects. In addition, it is necessary to set a notch filter of 50 Hz to remove the industrial frequency interference.

III. FEATURE SELECTION AND GESTURE RECOGNITION METHOD

A. sEMG Feature Extraction and Selection

sEMG is an analog signal collected from the surface of the human body with different characteristics in the time domain and frequency domain. There are a large number of publications investigating the influence of different features in the time domain, frequency domain and time-frequency domain on gesture recognition [16] [21]. In the following section, six features that act individually or in combination are used to recognize the hand gesture. They are three time-domain features: DAMV, IAV and VAR; one frequency-domain feature: AR; two time-frequency-domain features: DWTmax and DWTstd.

1) *DAMV*: the value of this feature indicates the vibration characteristics of the sEMG. The expression of DAMV is shown as follows:

$$DAMV = \frac{1}{N} \sum_{i=1}^{N-1} |x_{i+1} - x_i|. \quad (1)$$

2) *IAV*: this feature can reflect the level of muscle contraction. The expression of IAV is shown as below:

$$IAV = \frac{1}{N} \sum_{i=1}^N |x_i|. \quad (2)$$

3) *VAR*: this feature uses the magnitude of the sEMG as an eigenvalue. Since the DC component of sEMG has been removed in the data preprocessing, the average of sEMG can be regarded as zero. The expression of VAR is changed into the following form:

$$VAR = \frac{1}{N-1} \sum_{i=1}^N x_i^2. \quad (3)$$

In the above three equations, N is the length of sEMG time series, x_i is the i th sample amplitude of sEMG.

4) *AR*: The AR model considers the random signal sequence $x(n)$ as a response of a certain system stimulated by the white noise $w(n)$. Therefore, the parameters of the AR model can be used as the eigenvalues of the random signal. In this paper, the parameters in the fourth-order autoregressive model (AR4) are selected as the characteristics of sEMG. The expression of AR4 is as below:

$$x(n) = - \sum_{k=1}^4 a_k x(n-k) + w(n), \quad (4)$$

a_k is the parameter of AR4, $w(n)$ is Gaussian white noise.

5) *DWT*: The first step of wave transformation is to select a function as the fundamental wave which satisfies the integral is zero in the time domain. And then a discrete wavelet family $\psi_{ik}(t)$ which consists of member wavelets is obtained through the scale transformation and translation transformation of the fundamental wave $\varphi(t)$. It is defined as follows:

$$\psi_{ik}(t) = \frac{1}{\sqrt{2^i}} \varphi\left(\frac{t - k2^i}{2^i}\right), \quad (5)$$

i is the scale parameter, k represents the translation parameter. Then, the expression of Discrete Wavelet Transform can be defined as follows:

$$c_{i,k} = \frac{1}{\sqrt{2^i}} \int_{-\infty}^{+\infty} x(t) \varphi\left(\frac{t - k2^i}{2^i}\right) dt, \quad (6)$$

$c_{i,k}$ is the time-scale information of $x(t)$ after wavelet transforming.

In this paper, db5 wavelet is used to do 3 layers wavelet decomposition. The wavelet coefficients are extracted by the decomposed wavelet signal, and then the maximum or the standard deviation of the wavelet coefficients is extracted as the time-frequency domain feature of sEMG. The expressions of DWTmax and DWTstd are defined as below:

$$DWTmax = \max(x_i), \quad (7)$$

$$DWTstd = \sqrt{\frac{1}{N-1} \sum_{i=1}^N (x_i - \bar{x})^2}, \quad (8)$$

x_i is the wavelet coefficients matrix, \bar{x} is the average of x_i , and N is the length of x_i .

B. Gesture Recognition Using BP Neural Networks

After feature extraction and feature selection, some classifiers are used to classify the gesture through these features. In this paper, a three-layer BP neural network is used to do the hand gesture recognition. The number of input layer nodes n depends on the number of acquisition channels c and the number of features of the sEMG signal f . The relationship of these three variables is: $n = f \times c$.

When each channel uses a single feature such as DAMV, IAV, VAR as input, the number of input neurons is 5. When each channel uses AR4, DWTmax, DWTstd as input, the number of input neurons is 20. The number of output neurons is 8. The output of neurons in the output layer is between 0

TABLE I
BINARY CODES FOR EIGHT HAND GESTURES

Gestures	o_1	o_2	o_3	o_4	o_5	o_6	o_7	o_8
Fingers Extension	1	0	0	0	0	0	0	0
Fingers Flexion	0	1	0	0	0	0	0	0
Grasp a	0	0	1	0	0	0	0	0
Grasp b	0	0	0	1	0	0	0	0
Grasp c	0	0	0	0	1	0	0	0
Grasp d	0	0	0	0	0	1	0	0
Grasp e	0	0	0	0	0	0	1	0
Right-angle Hook	0	0	0	0	0	0	0	1

and 1. When using BP neural network to do the hand gesture recognition, the data set after feature extraction and selection is divided into two parts: 80% were used to train the neural network and 20% for the model test. In the training process, the output vector $o = (o_1, o_2, \dots, o_8)$ can be replaced by 8 binary codes shown in Table 1.

In the test process, in order to make the output to be either 0 and 1, the final output vector o should be transformed by the following trick:

$$o_i = \begin{cases} 1 & \text{if } o_i = \max\{o\}, i \in \{1, 2, \dots, 8\}, \\ 0 & \text{otherwise.} \end{cases} \quad (9)$$

The number of hidden layer neurons is 40. The hyperbolic tangent sigmoid function is chosen as the transfer function of neurons in then hidden layer. The transfer function of neurons in the output layer is the unit linear function.

IV. EXPERIMENTAL RESULTS AND ANALYSIS

A. Data Segmentation

Data segmentation is to divide the original data into several parts. The data in each segmentation is used to estimate signal features. A long length of segmentation can improve the accuracy of gesture classification, however, it increases the time consumption of data processing. A short length of segmentation can improve the processing speed and leaves sufficient time for calculating features, classifying gestures and real-time control of robots, however, it reduces the accuracy. It has been proved that the minimum interval between two distinct contractions is about 200 ms to estimate one hand gesture [16] [22]. Therefore, a study on the influence of data segmentation with different lengths has been investigated first. The optimal length of data segmentation should not only contain enough information to classify the hand gestures but also provide a reasonable time period for rehabilitation robots to achieve real-time control. The average classification accuracy under different lengths of data segmentation on 6 subjects is shown in Fig. 3.

For the time domain features DAMV and VAR, when the segmentation length is 250 ms, the accuracy rate reaches a value that is very close to the best result. For IAV, when the segmentation length is 500 ms, the accuracy is 93.4%, however, when the segmentation length is 250 ms, the accuracy can reach 91.72%. For the time-frequency domain features

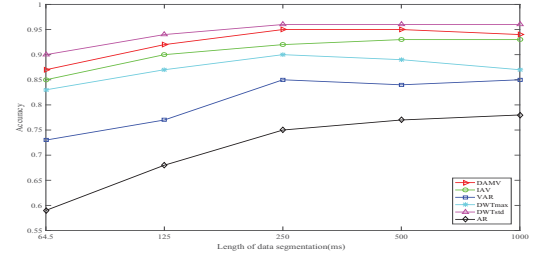


Fig. 3. Recognition rates with different single features and different lengths of data segmentation using BP neural network.

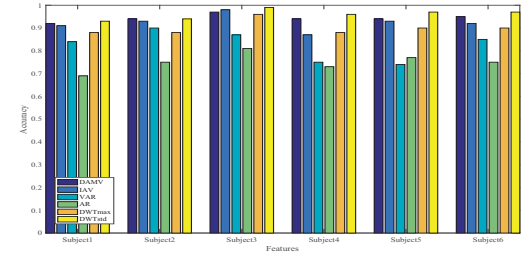


Fig. 4. Recognition rates with different single features of six volunteers using BP neural network.

DWTmax and DWTstd, the accuracy is also the best or very close to the best when the segmentation length is 250 ms. For the frequency domain feature AR, when the segmentation length is 250 ms, the accuracy is only 3% less than the best. These results show that when the data segmentation length is 250 ms, the extracted features can contain enough information to classify hand gestures and can leave enough time for the feature computation, gesture classification, and generation of control commands. Based on these observations, the data segmentation length is chosen to be 250 ms in the rest of experiments.

B. Recognition With Single Feature

The performance comparison of different single features on 6 subjects under BP neural networks is given in this experiment. The recognition results are shown in Fig. 4. DAMV, IAV and DWTstd have a similar performance, the accuracy rate can reach at least 90%. Among them, DWTstd obtains the highest recognition rate of 96.06%. For the features in the time domain, DAMV has the highest accuracy while the VAR has the lowest one. The frequency domain feature AR4 is worse than other features, the average accuracy rate is only 75%. For the time-frequency domain feature, DWTstd is better than DWTmax. By comparing the performance of different single features, DWTstd has the best accuracy, which is 96.06%.

C. Recognition With Multiple Features

It has been proved that the combination of some features as a multi-feature can effectively improve the recognition accuracy. However, the employment of the multi-feature increases the computing resource, which leads to the increase

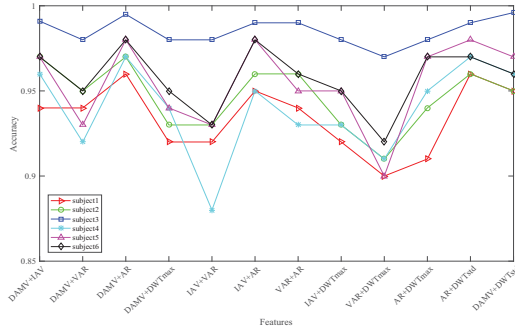


Fig. 5. Recognition rates with the two-feature combinations of six volunteers using BP neural networks.

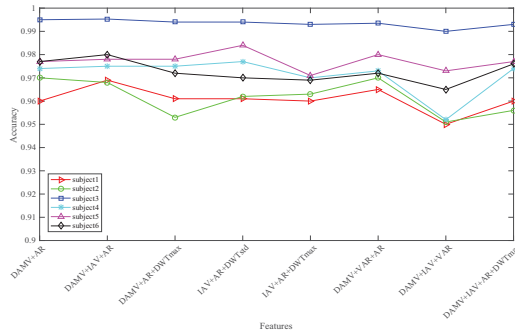


Fig. 6. Recognition rates with selected combinations of three or four features using BP neural networks.

of the recognition time. Therefore, this paper explores how to combine features to achieve a higher classification accuracy while maintaining the computation time at a reasonable level. The experiment results are shown in Fig. 5. From these results, it is demonstrated that the multi-feature combination has a better performance compared to the single feature case. The combination of the time domain feature and the frequency domain feature (AR) can obviously improve accuracy. For example, the combination of VAR and AR can reach to an accuracy of 95.25%, while the classification accuracy of using VAR or AR alone can only be 82.63% and 75%, respectively. Among all the two-feature combinations, The combination of DAMV and AR has a highest recognition rate of 97.02%.

The classification accuracy of three or four features combination was also explored. The recognition results are shown in Fig. 6. The combination of DAMV+IAV+AR wins the highest accuracy of 97.71%. It is a little bit higher than the combination of DAMV+AR which has best performance in the two-feature combination. The recognition rate of the other three feature combinations in this experiment can also reach to an accuracy above 97%. However, the combination of four features can not improve the recognition rate (the highest accuracy is 97.34%). Therefore, the combination of DAMV, IAV and AR under the BP neural network wins the best performance (the average accuracy is 97.71%).

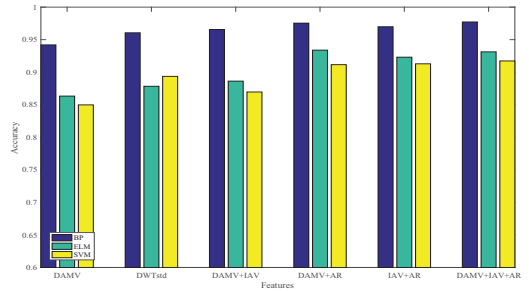


Fig. 7. Recognition rates under different classifiers with selected features.

D. Recognition With Different Classifiers

Classifiers are also crucial to the classification accuracy. An experiment aiming at comparing different classifiers (BP neural network, Extreme Learning Machine (ELM), Support Vector Machine (SVM)) has been developed. The activation function in ELM is the sigmoidal function and the number of hidden neurons is 3000. Radial basis function is selected to be the kernel function for the SVM classifier. The kernel parameter in SVM is 0.1 and the penalty parameter is 1.25. In this experiment, the classification performances of the above three classifiers are obtained under all single features and multi-features. Features with the satisfactory performance such as DAMV, DWTstd, DAMV+IAV, DAMV+AR, IAV+AR, DAMV+IAV+AR are shown in Fig. 7.

The results have demonstrated that DWTstd can win the best performance in different single features. As to the two-feature combination, DAMV+AR still has a very high classification accuracy. The best performance of ELM is achieved by DAMV+AR (the accuracy is only 93.4%). As to SVM, the highest accuracy is only 91.8% achieved by DAMV+IAV+AR. The results show that the BP neural network has a better performance than SVM and ELM. It is recommended to use the BP neural network together with the multi-feature DAMV+IAV+AR for the interaction between robots and patients because it has the best recognition rate of 97.71%.

V. CONCLUSIONS AND FUTURE WORK

In this paper, a study on the hand gesture recognition in Fugl-Meyer assessment scale using sEMG has been investigated and evaluated. This study aims at identifying the patients motion intention effectively and let the robot understand the patient's current recovery state to improve the quality of rehabilitation training. It has been found that the length of data segmentation, feature selection and feature combination can affect the accuracy of classification. The data segmentation length of 250 ms can not only contain enough information to classify the hand gestures but also provide a reasonable and effective time for rehabilitation robot to finish the real-time control. For the single-feature-based classification, DWTstd can reach a highest accuracy (i.e. 96%). Among all two-feature combinations, the champion is the combination of DAMV and AR whose classification accuracy is 97.5%. The best combination of three features can slightly improve the accuracy

to 97.71% (DAMV+IAV+AR). As to different classifiers, the BP neural network has a better performance than SVM and ELM. Based on experimental results, the following setting is recommended for the classification of hand gestures in Fugl-Meyer assessment scale: use the BP neural network as the classifier; use the “DAMV+IAV+AR” as the feature; and the length of data segmentation is 250 ms.

In the future, an attempt is to be made to realize the active rehabilitation in the robot platform. It uses the sEMG to identify the patient’s gestures first, and then takes the corresponding control strategy for different gestures. Furthermore, the control strategy requires the accurate and optimal control of fingers of patients. In order to realize the accurate control and task assignment of five fingers, some advanced control methods such as the model predictive control [23], [24], [25] and the distributed coordination control [26], [27], [28] can be employed. In addition, the sEMG can provide an objective and quantitative evaluation of the contraction sequence and degree of involvement of each muscle during the patient’s movement. Future study is also to focus on using sEMG to achieve an auxiliary assessment or automatic evaluation based on the Fugl-Meyer assessment scale.

REFERENCES

- [1] S. Mazzoleni, L. Puzzolante, L. Zollo, P. Dario, and F. Posteraro, “Mechanisms of motor recovery in chronic and subacute stroke patients following a robot-aided training,” *IEEE Transactions on Haptics*, vol. 7, no. 2, pp. 175-180, June 2014.
- [2] H.K. Yap, W.K. Benjamin, H.L. Jeong, C.H. James, and C.H. Yeow “A fabric-regulated soft robotic glove with user intent detection using EMG and RFID for hand assistive application,” in *Proceedings of the 2016 IEEE International Conference on Robotics and Automation*, Stockholm, Sweden, May 2016, pp. 3537-3542.
- [3] J.C. Metzger, O. Lamberg, A. Califfi, F.M. Conti, and R. Gassert, “Neurocognitive robot-assisted therapy of hand function,” *IEEE Transactions on Haptics*, vol. 7, no. 2, pp. 140-149, April-June 2014.
- [4] S.R. Soekadar, M. Witkowski, C. Gmez, E. Opisso, J. Medina, M. Cortese, M. Cempini, M.C. Carrozza, L.G. Cohen, N. Birbaumer, and N. Vitiello, “Hybrid EEG/EOG-based brain/neural hand exoskeleton restores fully independent daily living activities after quadriplegia,” *Science Robotics*, vol. 1, eaag3296, 2016.
- [5] D. Epstein, A. Mason, and A. Manca, “The hospital costs of care for stroke in nine European countries,” *Health Economics*, vol. 17, no. 1, pp. S21-S31, January 2008.
- [6] F. Zhang, Z.-G. Hou, L. Cheng, W. Wang, Y. Chen, J. Hu, M. Tan, and H. Wang, “iLeg-a lower limb rehabilitation robot: a proof of concept,” *IEEE Transactions on Human-Machine Systems*, vol. 46, no. 5, pp. 761-768, October 2016.
- [7] W. Wang, Z.-G. Hou, L. Cheng, L. Tong, F. Zhang, Y. Chen, L. Peng, L. Peng, and M. Tan, “Towards patients motion intention recognition: dynamics identification of a lower limb rehabilitation robot-an LLRR under motion constraints,” *IEEE Transactions on Systems, Man and Cybernetics: Systems*, vol. 46, no. 7, pp. 980-992, July 2016.
- [8] Hou. Li and L. Cheng, “Preliminary study on the design and control of a pneumatically-actuated hand rehabilitation device,” in *Proceedings of the 32nd Youth Academic Annual Conference of Chinese Association of Automation*, Hefei, China, May 19-21 2017.
- [9] L. Peng, Z.-G. Hou, L. Luo, L. Peng, W. Wang, and L. Cheng, “An sEMG-driven neuromusculoskeletal model of upper limb for rehabilitation robot control,” in *Proceedings of the 2016 IEEE Conference on Robotics and Biomimetics*, Qingdao, China, December 3-7 2016, pp. 1486-1491.
- [10] D. Zhang, Z.-G. Hou, L. Cheng, G. Bian, X. Xie, and L. Peng, “ ϵ -SVR-based estimation for the motion trajectory of human lower limb using acceleration signals,” in *Proceedings of the 2016 IEEE International Conference on Information and Automation*, Ningbo, China, July 2016, pp. 1278-1283.
- [11] J. Han, Q. Ding, A. Xiong, and X. Zhao, “A State-Space EMG model for the estimation of continuous joint movements,” *IEEE Transactions on Industrial Electronics*, vol. 62, no. 7, pp. 4267-4275, July 2015.
- [12] M.A. Harrach, B. Afsharipour, S. Boudaoud, V. Carriou, F. Marin, and R. Merletti, “Extraction of the Brachialis muscle activity using HD-sEMG technique and Canonical Correlation Analysis,” in *Proceedings of the 38th Annual International Conference of the IEEE Engineering in Medicine and Biology Society*, Orlando, United States, August 2016, pp. 2378-2381.
- [13] J. Winslow, A. Martinez, and C.K. Thomas, “Automatic identification and classification of muscle spasms in long-term EMG recordings,” *IEEE Journal of Biomedical and Health Informatics*, vol. 19, no. 2, pp. 464-470, March 2015.
- [14] Q. Ding, J. Han, X. Zhao, and Y. Chen, “Missing-data classification with the extended full-dimensional Gaussian Mixture Model: applications to EMG-based motion recognition,” *IEEE Transactions on Industrial Electronics*, vol. 62, no. 8, pp. 4994-5005, August 2015.
- [15] X. Zhai, B. Jelfs, H.M. Chan, and C. Tin, “Short latency hand movement classification based on surface EMG spectrogram with PCA,” in *Proceedings of the 38th Annual International Conference of the IEEE Engineering in Medicine and Biology Society*, Orlando, United States, August 2016, pp. 327-330.
- [16] Z. Ju, G. Ouyang, M.W. Korsak, and H. Liu, “Surface EMG based hand manipulation identification via nonlinear feature extraction and classification,” *IEEE Sensors Journal*, vol. 13, no. 9, pp. 3302-3311, September 2013.
- [17] G. Ouyang, X. Zhu, Z. Ju, and H. Liu, “Dynamical characteristics of surface EMG signals of hand grasps via recurrence plot,” *IEEE Journal of Biomedical and Health Informatics*, vol. 18, no. 1, pp. 257-265, January 2014.
- [18] A.A. Adewuyi, L.J. Hargrove, and T.A. Kuiken, “An analysis of intrinsic and extrinsic hand muscle EMG for improved pattern recognition control,” *IEEE Transactions on Neural Systems and Rehabilitation Engineering*, vol. 24, no. 4, pp. 485-494, April 2016.
- [19] F. Duan and L. Dai, “Recognizing the gradual changes in Semg characteristics based on incremental learning of wavelet neural network ensemble,” *IEEE Transactions on Industrial Electronics*, DOI: 10.1109/TIE.2016.2593693.
- [20] F. Zhang, P. Li, Z.-G. Hou, Z. Lu, Y. Chen, Q. Li, and M. Tan, “sEMG-based continuous estimation of joint angles of human legs by using BP neural network,” *Neurocomputing*, vol. 78, no. 1, pp. 139-148, February 2012.
- [21] B. Cesqui, P. Tropea, S. Micera, and H.I. Krebs, “EMG-based pattern recognition approach in post stroke robot-aided rehabilitation: a feasibility study,” *Journal of NeuroEngineering and Rehabilitation*, vol. 10, no. 75, pp. 1-15, July 2013.
- [22] M.A. Oskoei and H. Hu, “Support vector machine-based classification scheme for myoelectric control applied to upper limb,” *IEEE Transactions of Biomedical Engineering*, vol. 55, no. 8, pp. 1956-1965, August 2008.
- [23] W. Liu, L. Cheng, Z.-G. Hou, J. Yu, and M. Tan, “An inversion-free predictive controller for piezoelectric actuators based on a dynamic linearized neural network model,” *IEEE/ASME Transactions on Mechatronics*, vol. 21, no. 1, pp. 214-226, February 2016.
- [24] L. Cheng, W. Liu, Z.-G. Hou, J. Yu, and M. Tan, “Neural network based nonlinear model predictive control for piezoelectric actuators,” *IEEE Transactions on Industrial Electronics*, vol. 62, no. 12, pp. 7717-7727, December 2015.
- [25] L. Cheng, W. Liu, Z.-G. Hou, T. Huang, J. Yu, and M. Tan, “An adaptive Takagi-Sugeno model based fuzzy predictive controller for piezoelectric actuators,” *IEEE Transactions on Industrial Electronics*, vol. 64, no. 4, pp. 3048-3058, April 2017.
- [26] L. Cheng, Y. Wang, W. Ren, Z.-G. Hou, and M. Tan, “On convergence rate of leader-following consensus of linear multi-agent systems with communication noises,” *IEEE Transactions on Automatic Control*, vol. 61, no. 11, pp. 3586-3592, November 2016.
- [27] L. Cheng, Y. Wang, W. Ren, Z.-G. Hou, and Min Tan, “Containment control of multi-agent systems with dynamic leaders based on a PI²-type approach,” *IEEE Transactions on Cybernetics*, vol. 46, no. 12, pp. 3004-3017, December 2016.
- [28] L. Cheng, Z.-G. Hou, and M. Tan, “A mean square consensus protocol for linear multi-agent systems with communication noises and fixed topologies,” *IEEE Transactions on Automatic Control*, vol. 59, no. 1, pp. 261-267, January 2014.